SIMULATED EARTHQUAKE MOTIONS
FOR DESIGN PURPOSES

by

P. C. Jennings[I], G. W. Housner[II] and N. C. Tsai[III]

SYNOPSIS

Simulated earthquake motions suitable for design calculations are generated on a digital computer. The accelerograms are sections of a random process with a prescribed power spectral density, multiplied by envelope functions to give the desired variation in intensity with time. Two each of four types of accelerograms have been generated. Type A models the maximum ground motion in a Magnitude 8 shock and type B the maximum motion expected in a Magnitude 7 earthquake. The shaking expected in the epicentral area of a Magnitude 5 or 6 earthquake is modeled by type C and the motion close to the fault in a shallow Magnitude 4 or 5 shock is represented by type D. Accelerograms, derived velocity and displacement curves, and response spectra are included in the presentation.

INTRODUCTION

In the earthquake design of important structures it is not uncommon for a digital computer analysis to be made of the response of the structure to a prescribed base acceleration. Recorded earthquake accelerograms are often used for this purpose even though these might not have completely suitable properties. For example, the El Centro, 1940, accelerogram has been used all over the world even though its special character is not really applicable. Because of the rarity of strong earthquakes, the localized extent of the really strong ground shaking, and the seeming proclivity of earthquakes to occur in uninstrumented areas, there are wide gaps in the present-day collection

---

[I] Associate Professor of Applied Mechanics, California Institute of Technology, Pasadena, California.

[II] Professor of Civil Engineering and Applied Mechanics, California Institute of Technology.

[III] Graduate Student, California Institute of Technology.

of strong-motion accelerograms. The most significant gap is that the shaking in the vicinity of the causative fault in a truly great ,Richter Magnitude 8) earthquake has never been recorded. Also, only three recordings in the epicentral regions of Magnitude 7 earthquakes have been made in the United States (El Centro, California, 1940, Olympia, Washington, 1949 and Taft, California, 1952). The statistical fluctuations in intensity, duration and frequency content in these records and records of comparable earthquakes from Mexico and South America indicate that a much larger sample of strong earthquake motion is needed to define completely the characteristics of strong ground shaking. This is also true of damaging, or potentially damaging shocks of lesser Magnitudes (Richter Magnitude 4 or greater).

Because many years will be required to assemble collections of records of different types, research workers have generated ensembles of simulated earthquakes by various means to help fill the gaps in record d data. The models for these simulated motions are deduced from examination of the statistical properties of recorded accelerograms, the most significant of which are the duration, intensity and frequency content of the motion. The intensity and frequency content are, in general, functions of time.

Mathematical models of varying complexity have been used or suggested to model accelerograms. These models include a white noise (1, 2, 3, 4) stationary Gaussian Processes (5, 6, 7) and nonstationary processes of various types (8, 9, 10, 11, 12).

All of the proposed types of statistical models embody some of the important properties of strong ground motion and the choice of the model to be used depends on the characteristics that are important to the problem at hand. Thus, many of the characteristics of the response of linear, damped structures to earthquake motions can be modeled by the response to white noise (4) but the frequency content of this model is known to be inaccurate. Housner and Jennings (6) showed that the key central portion of the acceleration from strong earthquakes could be modeled by sections of a stationary Gaussian process with a spectral density derived from average undamped velocity spectra. Although satisfactory for most response studies, the artificial earthquakes generated by this process are not appropriate for modeling smaller earthquake motions or for use in studies where the less intense but longer tails of the accelerograms are thought to be significant. An important example is in studies of the tendency of certain soils to liquefy under cyclic straining(13).

To model the shaking in smaller earthquakes (Richter Magnitude of 5 or 6) and to model the tail of larger shocks it is necessary to employ a nonstationary random process. One of the simplest types of nonstationary processes consists of a stationary process multiplied by a time-dependent envelope function (14). Amin and Ang (11) have shown that a filtered Poisson process modified by such an envelope is a satisfactory model for motions expected during large earthquakes. To model the rapid build-up of motion, the central portion of strong shaking,

146

A-1

and the decaying tail, Amin and Ang use an envelope function divided into three parts: a) a rapid quadratic build-up in intensity from zero; b) a constant central portion; and c) an exponentially decaying tail.

In the work reported here, the nonstationarity of the accelerogram also is introduced by envelope functions of this general type, but the envelope functions are applied to sections of the same Gaussian random process used previously to model the central portion of strong earthquakes (6). The present work also differs from previous efforts in that attention is focused on the preparation of simulated earthquake motions appropriate for use in design calculations of special structures. For this purpose, two each of four different types of accelerograms have been generated to represent ground acceleration in a variety of earthquakes ranging from a great earthquake, such as occurred in Chile in 1960 or Alaska in 1964, to a small, close shock such as recorded in Parkfield, California in 1966. The accelerograms have been processed, filtered, and scaled to have the properties appropriate to the ground motion they model.

The two accelerograms of each type are intended to serve as two components of the same shock for calculations of two-dimensional motion, or as two independent samples of possible ground shaking in the same type of event. The presentation in this report includes the accelerograms and derived velocity and displacement curves as well as response spectra. Card decks, giving the acceleration ordinates at 1/40 second intervals, will be furnished on request to persons interested in making calculations using these simulated motions.

The simulated earthquake accelerograms have been scaled to represent ground shaking close to the causative fault, but they can be modified to represent different conditions. For example, by changing the time scale the frequency content can be changed, and the amplitude scale can also be changed. The intensity and duration of accelerograms A-1 and A-2 were established by extrapolating from recorded smaller earthquakes and it is thought that A-1 and A-2 represent an upper bound for intensity and duration of ground shaking for earthquakes of Magnitudes 8 to 8.5.

GENERATION OF EARTHQUAKE MOTION

Consider a stationary random process $\{\ddot{x}(t)\}$ which can be taken to be normally distributed with a mean of zero and a variance of unity. Each member, $\ddot{x}(t)$, has the units of acceleration. Let $E(t)$ be the envelope function which describes the manner in which the intensity of the desired nonstationary process varies with time. Members of a nonstationary ensemble $\{\ddot{z}_1(t)\}$ then can be defined by

$$\ddot{z}_1(t) = E(t)\ddot{x}(t) \tag{1}$$

It follows from the properties of $\{\ddot{x}(t)\}$ that $\{\ddot{z}_1(t)\}$ will be Gaussian with mean zero and variance $E^2(t)$. The duration of the nonstationary process is prescribed by letting $E(t)$ be non-zero only over a fixed time interval.

In general, the frequency characteristics of $\{\ddot{z}_1(t)\}$ will depend both on $E(t)$ and $\{\ddot{x}(t)\}$. However, if $E(t)$ varies slowly with respect to the frequencies of interest, the frequency content of $\{\ddot{z}_1(t)\}$ will be determined primarily by $\{\ddot{x}(t)\}$. This will occur, for example, if $E(t)$ has a constant value over a major fraction of the interval for which it is non-zero.

For this work, $\{\ddot{x}(t)\}$ is the stationary process designed to model the strong central portion of the accelerograms recorded during strong earthquakes (6). In reference 6 it was shown that accelerograms which are portions of this random process produced response spectra and ground velocity and displacement curves which resembled closely corresponding results for real earthquake motions. The frequency content of the process was selected so the average spectra of the real and artificial earthquakes matched closely. The details of the generation of $\{\ddot{x}(t)\}$ are available in the literature (6,15) and will not be repeated here. In essence the process $\{\ddot{x}(t)\}$ is generated by passing a Gaussian white noise through a second-order linear filter (one degree of freedom oscillator) which determines the power spectral density of the resulting output. The spectral density was taken from a relation shown to exist between the power spectral density of $\{\ddot{x}(t)\}$ and the average undamped velocity spectra of four of the strongest earthquake motions so far recorded in the western United States.

Therefore, the process $\{\ddot{z}_1(t)\}$ already contains many of the characteristics desired for the simulated accelerograms, and the primary purpose of the envelope function $E(t)$ in Equation 1 is to specify further how the intensity of the acceleration varies with time, from an initial build-up of intensity to the final decay to a negligible value.

Four envelope functions $E(t)$ were selected to model four different types of earthquake motion which are thought to be of significance for engineered structures. The four kinds of motion are labeled type A, B C, and D. The envelope functions for type A is shown in Fig. 1; the other envelopes are of the same general type. Because of Eq. 1, a plot $E(t)$ shows the relative magnitude of the standard deviation of $\{\ddot{z}_1(t)\}$ as a function of time.

Earthquake Type A is of 120 seconds total duration and is designed to represent an upper bound for the ground motions expected in the vicinity of the causative fault during an earthquake having a Richter Magnitude of 8 or greater. Such motion has not yet been recorded but studies have shown (16) that such motions should have many of the properties exhibited by the type A accelerograms. Type B motion has a duration of 50 seconds and is intended to model the shaking close to the

148

fault in a Magnitude 7 earthquake, such as occurred in El Centro, California in 1940 and in Taft, California in 1952.

The duration of earthquake C is 12 seconds; this type of simulated motion models that expected in the epicentral region of a Magnitude 5.5 to 6 shock, such as occurred in San Francisco in 1957 and in Helena, Montana in 1935. In highly seismic regions such shocks could occur several times in the life of a structure. Earthquake type D, with a duration of 10 seconds, and a much smaller duration of strong shaking, is intended to model the shaking quite close to the fault in a very shallow Magnitude 4.5 to 5.5 earthquake. Such a shock was recorded at several stations in Parkfield, California in 1966; the most remarkable features of the accelerogram recorded 200 ft from the fault were that the maximum acceleration was 50 percent g and the duration of strong motion was 1.5 seconds (17).

In common with most recorded strong-motion accelerograms, the process $\{\ddot{z}_1(t)\}$ from Equation 1 does not have a reasonable baseline, as evidenced by the behavior of the integrated ground velocity $\{\dot{z}_1(t)\}$. Figures 2(a) and 2(b) give $\ddot{z}_1(t)$ and $\dot{z}_1(t)$ for earthquake C-1 and show the ground velocity positive for the later half of the record and trending to a non-zero value at the end of the excitation. Such behavior is not realistic and is eliminated by a small adjustment of the acceleration baseline in the same manner used to adjust the same trend in real accelerograms (18). The adjusted accelerogram and the derived velocity for earthquake C-1 are shown in Figures 2(c) and (d), which show that the effect of the adjustment on the acceleration is almost indiscernible, and that the higher frequency content of the ground velocity is not altered

The correction to the accelerogram $\ddot{z}_1(t)$ takes the form of a parabolic addition to the baseline. Thus, the modified acceleration $\ddot{z}_2(t)$ is given by

$$\ddot{z}_2(t) = \ddot{z}_1(t) + a_1 + a_2 t + a_3 t^2 \qquad (2)$$

It was found that the magnitude of the coefficients a_i were usually proportional to the duration of the accelerogram. Hence, a_1, the small nonzero start of the accelerogram $\ddot{z}_2(t)$, was larger for types A and B than for the shorter C and D types. The magnitude of a_1 for earthquake C-1 is shown in Figure 2(c). Because accelerograms starting from zero were desired, this feature was removed by a linear correction of one second duration for types A and B and 1/2 second duration for types C and D. As can be judged from Figure 2(c), the effect of a linear correction applied to the first half-second of earthquake C-1 would have a negligible effect on the accelerogram, and therefore a corresponding negligible effect on the spectra calculated from the acceleration. The effects of this correction on the ground velocity and displacement are not negligible but are over-ridden by the effects of subsequent filtering.

Designating the acceleration after the least-square modification and the correction at the beginning of the motion as $\ddot{z}_3(t)$, this acceleration

A-1

was then filtered to give a frequency content, as judged by response spectra and ground velocity and displacement curves, appropriate to the motions which were modeled. The filter used was a second-order linear filter which corresponds physically to a one degree of freedom oscillator. The input at the base is $-\ddot{z}_3(t)$ and the filtered output is the relative acceleration $\ddot{z}(t)$.

The effect of this filter can be seen by examining its equation of motion.

$$\ddot{z} + 2n_f\omega_f\dot{z} + \omega_f^2 z = \ddot{z}_3(t) \tag{3}$$

Equation 3 implies that if ω_f is small compared to the component of $\ddot{z}_3(t)$ at a particular frequency, then in this frequency range $\ddot{z}(t) \approx \ddot{z}_3(t)$. Conversely, for excitation with low frequency compared to ω_f , the mass moves with the base and $\ddot{z}(t)$ is much smaller than $\ddot{z}_3(t)$.

The behavior described above can be examined mathematically by comparing the relative steady-state response to sinusoidal excitation at various frequencies. This response, called the transfer function, is the ratio of the steady-state magnitudes of $\ddot{z}(t)$ and $\ddot{z}_3(t)$, for the special case in which the excitation is

$$z_3(t) = A \sin \omega t \tag{4}$$

The transfer function is found to be

$$T_r\left(\frac{\omega}{\omega_f}, n_f\right) = \frac{\left(\frac{\omega}{\omega_f}\right)^2}{\sqrt{\left[1 - \left(\frac{\omega}{\omega_f}\right)^2\right]^2 + \left[2n_f\frac{\omega}{\omega_f}\right]^2}} \tag{5}$$

To avoid an undesirable resonance for frequency components near ω_f , the damping of the filter must be rather large and it is easily shown that particularly good performance is achieved if $n_f = 1/\sqrt{2}$. Substituting in Equation 5 and expressing the results in terms of the period yields

$$T_r\left(\frac{T}{T_f}\right) = \frac{1}{\sqrt{1 + \left(\frac{T}{T_f}\right)^4}} \tag{6}$$

From Equation 6 it can be shown that the filter passes essentially unmodified periodic components less than T_f, whereas components exceeding T_f are greatly diminished so that it functions as a low-pass filter.

The diminution of the longer period components of the simulated earthquake motions can be seen from a comparison of the spectra of $\ddot{z}_2(t)$ in Figure 3(a) and of $\ddot{z}(t)$ in Figure 3(b). Again this illustrative example is for earthquake C-1. In this case the natural period of the filter used was two seconds, and the rapid decrease in the spectra of the filtered motion for periods greater than two seconds shows up clearly. Also Figure 3 shows that the effect of the filter decreases rapidly for periods progressively shorter than two seconds.

The values of T_f used for the different types of simulated earthquakes were chosen primarily on the basis of the response spectra of the filtered motion for the shorter earthquakes and on the basis of the frequency content of the ground velocity and displacement for the larger earthquakes. On these bases, the values of T_f were chosen to be two seconds for earthquake types C and D and seven seconds for earthquake types A and B. Real earthquakes of 120 or 50 seconds duration may well have period components larger than about seven seconds, but the acceleration associated with the frequency of motion appears to be so low that it cannot be recorded accurately by existing strong-motion accelerographs. Therefore, it was judged appropriate that they be diminished greatly. The choice of seven seconds as the filter frequency is, of course somewhat arbitrary, but gave acceptable results. For response spectra calculated for periods up to four seconds, this filtering has no appreciable effect.

It is noteworthy that the response spectra for the shorter simulated earthquakes tend to come together for large values of T, for example in Figure 3(b). This effect also has been observed for spectra of real earthquakes of this duration and illustrates the well-known fact that for large periods the maximum value of the displacement of the simple oscillator used to calculate spectra must eventually approach the maximum value of the ground displacement.

To complete the generation of the simulated earthquakes, they must be scaled to intensities representative of the earthquakes they are intended to model; heretofore in the generation process the scale of the accelerograms has been arbitrary. For earthquake types A B and C, the basis of the scaling was the average of the 20 percent damped spectrum intensity of the two records of each type. For earthquake type D, the maximum acceleration was used.

The 20 percent damped spectrum intensity is defined as (19)

$$SI_{0.20} = \int_{0.1}^{2.5} S_v(0.20, T)dT \qquad (7)$$

in which S_v is the velocity spectra as a function of period T. In this presentation the integral of Equation 7 was evaluated using ωS_d rather than S_v; this substitution is not expected to be significant over the period range involved in Equation 7 (20).

The accelerograms of earthquake type A were scaled so that the average value of the spectrum intensity is 150 percent as strong as the average spectrum intensity of the two components of the El Centro, 1940 record. Earthquake type B was scaled so the average spectrum intensity would equal the average spectrum intensity of the El Centro, 1940 record. The average intensity of the two earthquakes of type C was set equal to the average of the two components recorded at Golden Gate Park, San Francisco, during the 1957 earthquake. The scale factor needed to produce the required intensities for the simulated motion is just the ratio of spectrum intensity of the appropriate real earthquake to the spectrum intensity of the simulated motion as generated.

Earthquake type D is intended to model the motion recorded very close to the causative fault in a small earthquake. For this motion the spectrum intensity does not measure well the scale of the motion and the maximum acceleration was used instead. For the two earthquakes of type D, the maximum acceleration was scaled to be 0.50g, the maximum acceleration recorded in the Parkfield, California shock (21).

Table I summarizes the primary characteristics of the various types of simulated earthquake motions and includes the duration of the strong central portion of the envelope function E(t) ; the period of the system used to filter the motion; the spectral intensities of the unscaled motion; and the scale factors needed to bring the motion up to the desired intensity The absolute values of the scale factors have little meaning, but the relative values needed to produce the desired motions give some insight into the scaling process.

Some idea of the statistical fluctuations in the simulated motions can be found also from Table I. The variation of the spectrum intensity between two motions of the same type is about the same as has been observed between two horizontal components of the same earthquake motion.

The accelerograms can, of course, be scaled as desired to represent various intensities of shaking, and by a change of time-scale can be made to represent ground motions with different frequency content. For example, by a 2 to 1 change of time-scale, earthquake A-1 can represent 60 seconds of higher frequency ground motion with 40 percent g maximum acceleration, a record similar to the accelerogram recorded in Lima, Peru, 17 October 1966.

PRESENTATION OF RESULTS

Earthquake accelerograms of each type in their final form are presented together with the velocity and displacement curves in Figures 4 through 7 wherein it should be noted that the time scales are different for the different types of motion.

Response spectra for the accelerograms shown in Figures 4 to 7 are plotted in Figures 8 to 11. The spectra given are ωS_d plotted as a

A-1

function of period. These spectra have nearly all the properties of velocity spectra and have been called the "Pseudo-velocity spectra." Their advantage over the velocity spectra lies in the fact that division of the spectrum value by ω produces the exact value of the maximum displacement, and multiplication by ω produces the exact value of the maximum shear force per unit mass. Similar operations on the velocity spectra are only approximately true and are not always satisfactory.

SUMMARY AND CONCLUSIONS

The simulated earthquakes are intended to model four types of strong earthquake motions and have been shaped and scaled accordingly. The two motions of each kind can be used to model the horizontal components of the same shock, or to represent a repetition of the same type of earthquake.

Type A models the shaking in the vicinity of the fault in a great (Richter Magnitude 8 or greater) earthquake, and has a spectrum intensity 150 per cent stronger than the El Centro, 1940 shock. Earthquakes of Type B represent the strong shaking in a Magnitude 7 or greater earthquake, and have the same spectrum intensity as the El Centro, 1940 record. The earthquakes of Type C model the shaking expected in the epicentral region of a Magnitude 5.5 to 6 earthquake, and have the same average intensity as the record obtained at Golden Gate Park during the 1957 San Francisco earthquake. For earthquakes of Type D, which model the shaking close to the fault in a shallow Magnitude 4.5 to 5.5 earthquake, the motions have been scaled to have a maximum acceleration of 50 per cent g, the maximum recorded in the Parkfield, California earthquake of 1966.

It is concluded that the simulated earthquakes are reasonably representative of the type of motions modeled, and from the generation process it is concluded that most of the characteristics of strong ground motion records obtained on firm ground can be modeled by simple random processes and the statistical fluctuations which are inherent in such processes.

The eight artificial earthquakes were generated to augment the number of accelerograms available for use in digital response studies of structures and copies or listings of the acceleration decks, consisting of acceleration ordinates at 1/40 second intervals, will be made available upon request.

ACKNOWLEDGMENT

BIBLIOGRAPHY

1. Housner, G. W., "Characteristics of Strong-Motion Earthquakes, " Bull. Seis. Soc. Amer., 37, 1, Jan. 1947.

2. Rosenblueth, E., "Some Applications of Probability Theory in Aseismic Design, "Proc. World Conf. on Earthq. Eng., Berkeley, Calif., June, 1956.

3. Rosenblueth, E. and Bustamante, J. E., "Distribution of Structural Response to Earthquakes, "Jour. Engrg. Mech. Div., ASCE, 88, EM3, June, 1962.

4. Bycroft, G. N., "White Noise Representation of Earthquakes, "Jour. Engrg. Mech. Div., ASCE, 86, EM2, Apr. 1960.

5. Tajimi, H., "A Statistical Method of Determining the Maximum Response of a Building Structure During an Earthquake, "Proc. Second World Conf. on Earthq. Engrg., Vol. II, Tokyo, July, 1960.

6. Housner, G. W. and Jennings, P. C., "Generation of Artificial Earthquakes, "Jour. Engrg. Mech. Div., ASCE, 90, EM1, Feb. 1964.

7. Barstein, M. F., "Application of Probability Methods for Designing the Effect of Seismic Forces on Engineering Structures, "Proc. Second World Conf. on Earthq. Engrg., Vol. II, Tokyo, July, 1960.

8. Bolotin, V. V., "Statistical Theory of Aseismic Design of Structures, " Ibid.

9. Bogdanoff, J. L., Goldberg, J. E., and Bernard, M. C., "Response of a Simple Structure to a Random Earthquake-Like Disturbance, "Bull. Seis. Soc. of Amer., 51, 2, Apr. 1961.

10. Cornell, C. A., "Stochastic Process Models in Structural Engineering, ' Tech. Report 34, Stanford Univ. Dept. of Civil Engrg., May, 1964.

11. Amin, M., and Ang, A. H. -S., "A Nonstationary Stochastic Model for Strong-Motion Earthquakes, "Struct. Res. Series 306, Univ. Ill. Dept. Civil Engrg., Apr. 1966.

12. Shinozuka, M., and Sato, Y., "Simulation of Nonstationary Random Processes, "Jour. Engrg. Mech. Div. ASCE, 93, EM1, Feb., 1967.

13. Seed, H. B. and Wilson, S. D., "The Turnagain Heights Landslide In Anchorage, Alaska, "Dept. of Civ. Engrg., Univ. Calif., Berkeley.

14. Bendat, J. S. and Piersol, A. G., Measurement and Analysis of Random Data, Wiley & Sons, New York, 1966.

15. Jennings, P. C., "Response of Simple Yielding Structures to Earthquake Excitation, "Earthq. Engrg. Res. Lab., Calif. Inst. of Tech., Pasadena, 1963.

16. Housner, G. W., "Intensity of Earthquake Ground Shaking Near the Causative Fault, "Proc. Third World Conf. on Earthq. Engrg., Vol. I, Auckland and Wellington, Jan. 1965.

17. Housner, G. W. and Trifunac, M. D., "Analysis of Accelerograms-Parkfiel Earthquake, "Bull. Seis. Soc. Amer., 57, 6, Dec. 1967.

18. Berg, G. V. and Housner, G. W., "Integrated Velocity and Displacement of Strong Earthquake Ground Motion, "Bull. Seis. Soc. Amer., 51, 2, Apr. 1961.

19. Housner, G. W. , "Spectrum Intensities of Strong Motion Earthquakes," Proc. Symp. on Earthq. and Blast Effects on Struct. , Earthquake Engrg. Res. Inst. , 1952.

20. Hudson, D. E. , "Some Problems in the Application of Spectrum Techniques to Strong-Motion Earthquake Analysis, " Bull. Seis. Soc. Amer. , 52, 2, Apr, 1962.

21. Cloud, W. K., and Perez, P. , "Accelerogram — Parkfield Earthquake, " Bull. Seis. Soc. Amer. , 57, 6, Dec. 1967.

22. Jennings, P. C. , Housner, G. W. and Tsai, N. C. , "Simulated Earthquake Motions, " Earthq. Engrg. Res. Lab. , Calif. Inst. of Tech. , Pasadena, 1968.
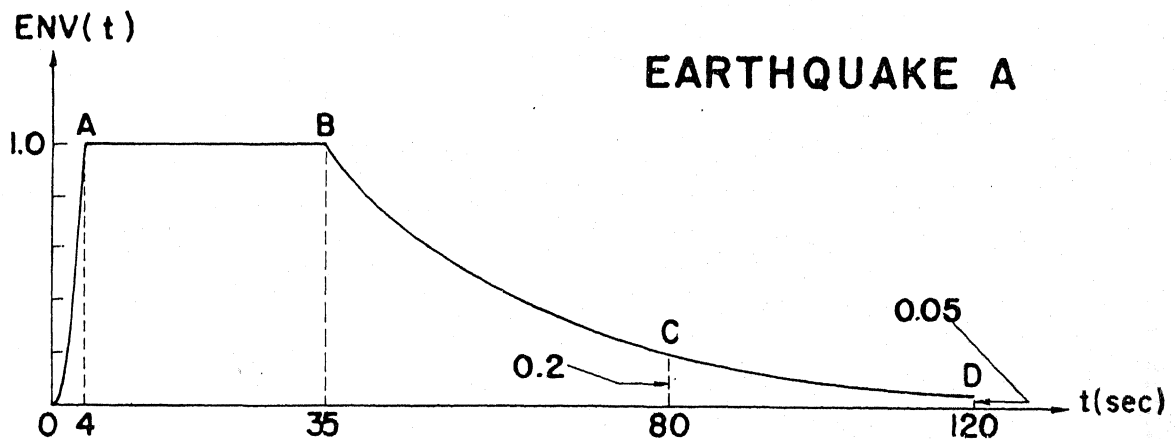
ENV(t)

EARTHQUAKE A

$$OA : ENV(t) = t^2/16$$
$$AB : 1.0$$
$$BC : exp(-0.0357(t-35))$$
$$CD : 0.05 + 0.0000938(120-t)^2$$

FIG. 1 - ENVELOPE FUNCTION FOR EARTHQUAKE TYPE A

A-1
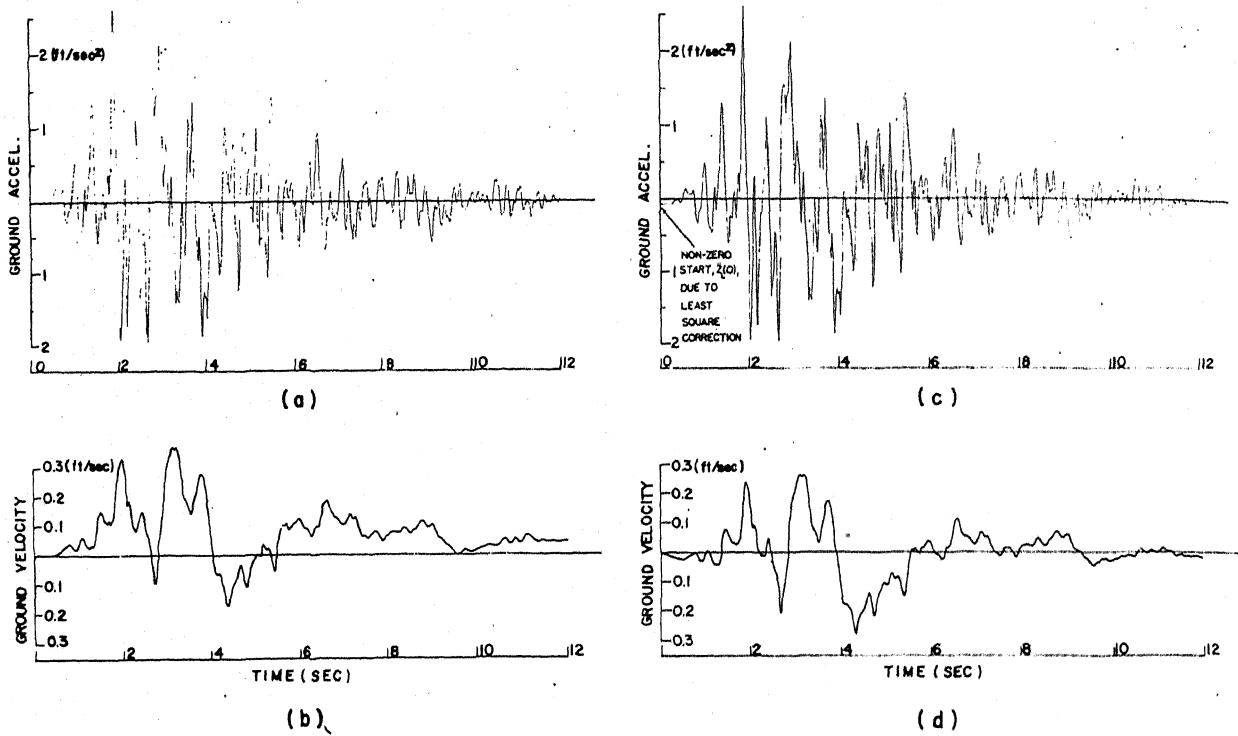
FIG. 2 - EFFECTS OF LEAST SQUARE ADJUSTMENT ON
EARTHQUAKE C-1. a) UNADJUSTED ACCELERATION;
b) UNADJUSTED VELOCITY; c) ADJUSTED ACCELERA-
TION; AND d) ADJUSTED VELOCITY.
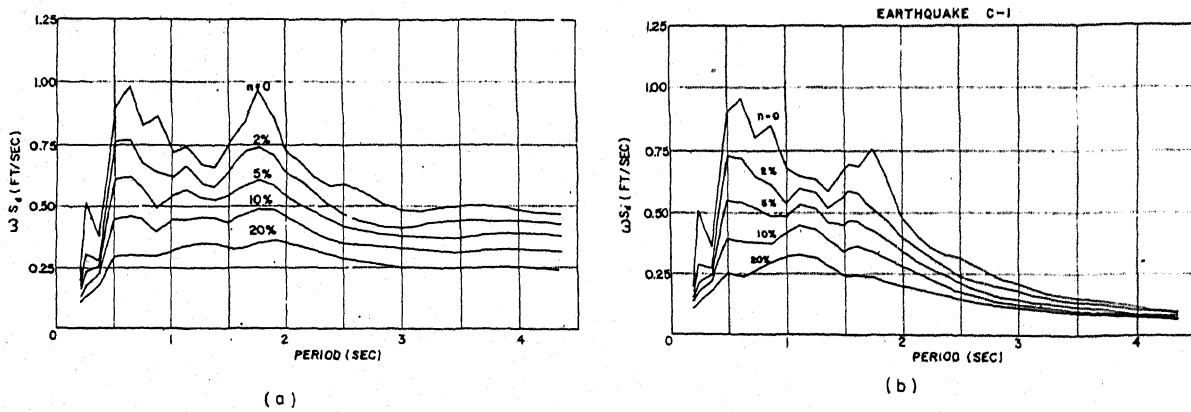
FIG. 3 - EFFECTS OF FILTERING ON THE SPECTRUM OF
EARTHQUAKE C-1. a) BEFORE FILTERING; AND
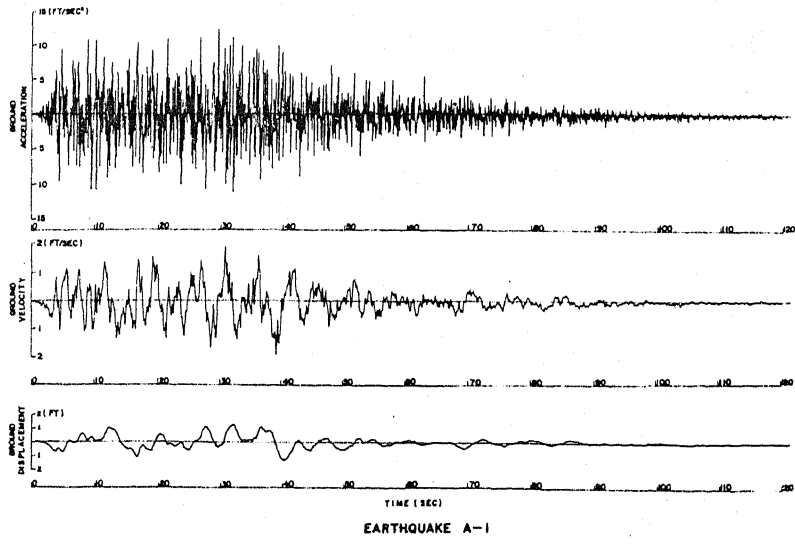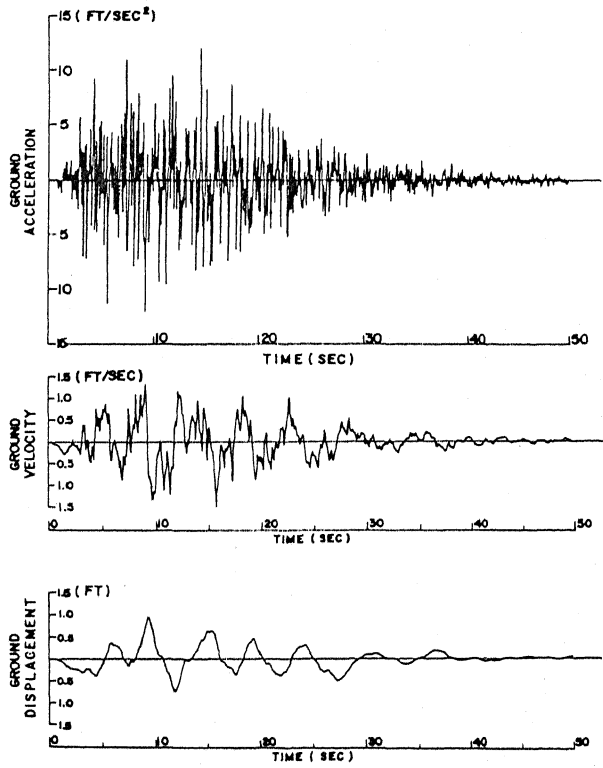b) AFTER FILTERING WITH $T_f = 2$ SECONDS.

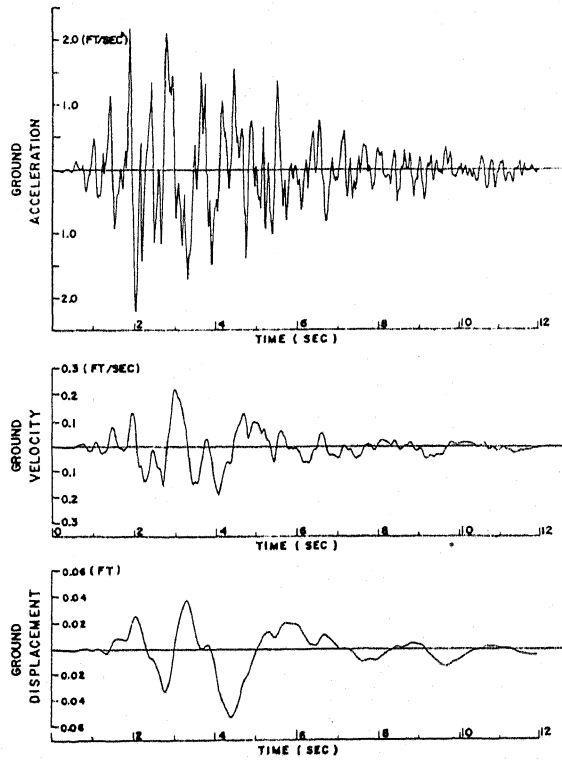156   A—1

EARTHQUAKE A-I

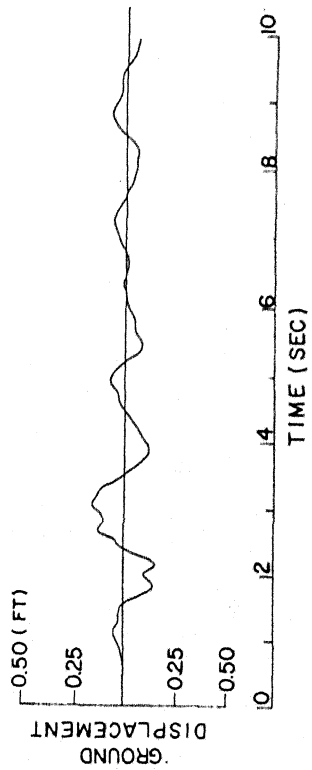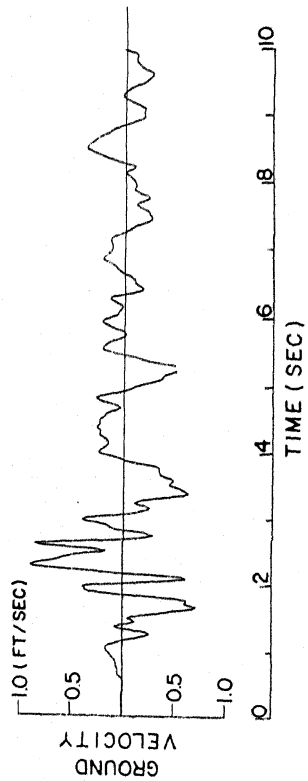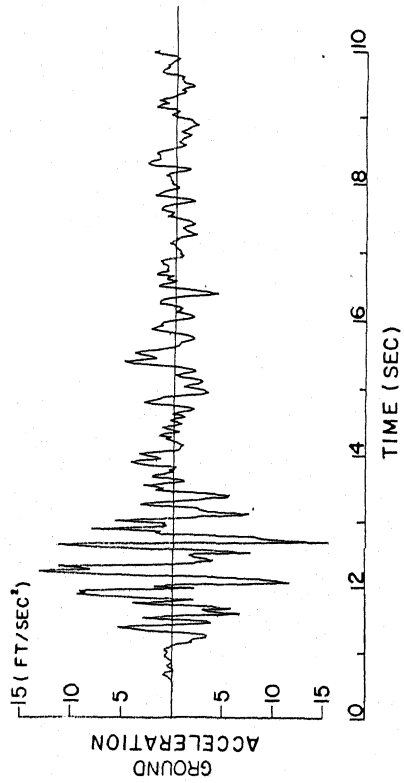FIG. 4 - ACCELERATION, VELOCITY AND DISPLACEMENT
FOR EARTHQUAKE A-1

EARTHQUAKE B-I

EARTHQUAKE C-I

FIG. 5 - ACCELERATION VELOCITY AND DISPLACEMENT
FOR EARTHQUAKE B-1

FIG. 6 - ACCELERATION, VELOCITY AND DISPLACEMENT
FOR EARTHQUAKE C-1

A-1

EARTHQUAKE A-1

ωS_d SPECTRUM FOR EARTHQUAKE A-1

n = 0%
2%
5%
10%
20%

PERIOD (SEC)

ωS_d (FT/SEC)

FIG. 8 - ωS_d SPECTRUM FOR EARTHQUAKE A-1

EARTHQUAKE B-1

n=0
n=2%
n=5%
n=10%
n=20%

PERIOD (SEC)

ωS_d (FT/SEC)

FIG. 9 - ωS_d SPECTRUM FOR EARTHQUAKE B-1

GROUND ACCELERATION
15 (FT/SEC²)
10
5
5
10
15

GROUND VELOCITY
1.0 (FT/SEC)
0.5
0.5
1.0

GROUND DISPLACEMENT
0.50 (FT)
0.25
0.25
0.50

TIME (SEC)

EARTHQUAKE D-1

FIG. 7 - ACCELERATION, VELOCITY AND DISPLACEMENT FOR EARTHQUAKE D-1
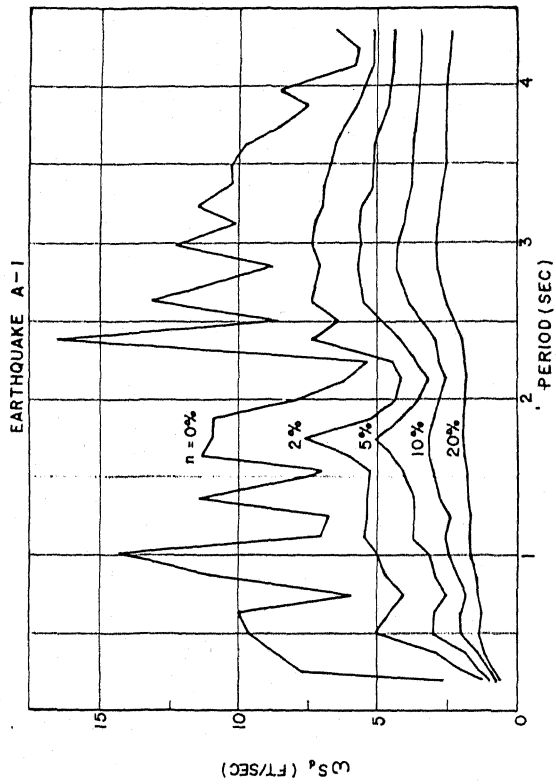
158

A-1

FIG. 10 - ωS_d SPECTRUM FOR EARTHQUAKE C-1
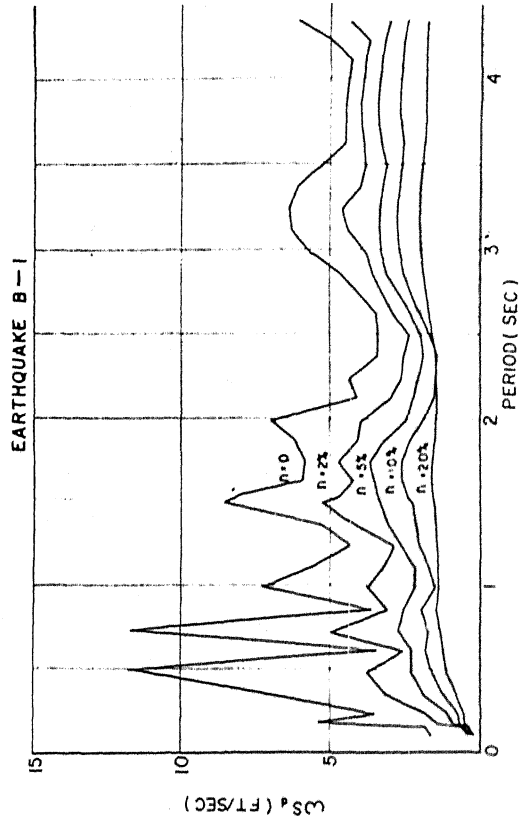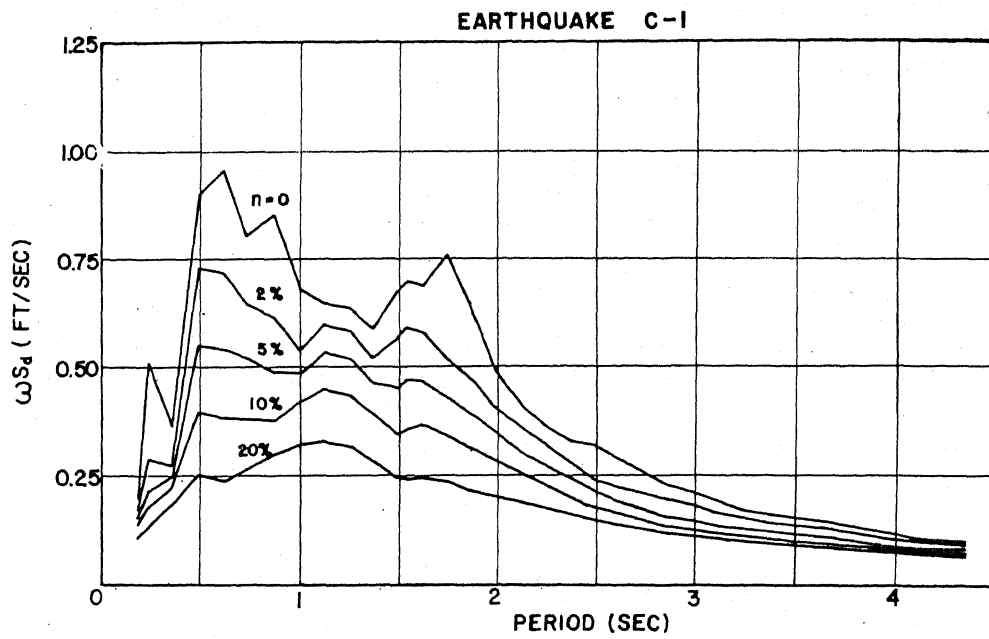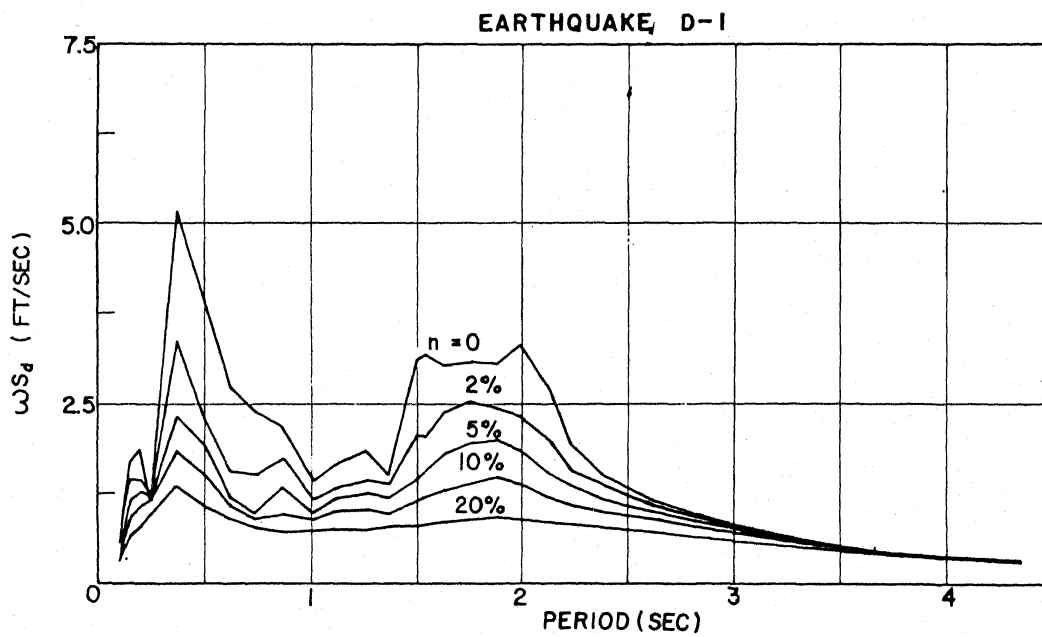

FIG. 11 - ωS_d SPECTRUM FOR EARTHQUAKE D-1

A-1

TABLE I

SUMMARY OF PROPERTIES OF SIMULATED EARTHQUAKES

(1)	(2)	(3)	(4)	(5)	(6)
Simulated Earthquake Type	Total Duration (sec)	Duration of the Strong Motion Portion with Constant Envelope (sec)	Filter Period T_f (sec)	Unscaled Damped Spectrum Intensity	Scale Factor to Produce Final Motion
A	120	29	7	0.409 (A-1) 0.420 (A-2)	9.21
B	50	11	7	0.330 (B-1) 0.244 (B-2)	9.44
C	12	2	2	0.354 (C-1) 0.271 (C-2)	1.56
C	10	0.5	2		20 (D-1) 16 (D-2)

A-1